We are IntechOpen,
the world's leading publisher of
Open Access books
Built by scientists, for scientists

4,800
Open access books available

122,000
International authors and editors

135M
Downloads

Our authors are among the

154
Countries delivered to

TOP 1%
most cited scientists

12.2%
Contributors from top 500 universities

CLARIVATE ANALYTICS

BOOK CITATION INDEX

INDEXED

WEB OF SCIENCE™

Selection of our books indexed in the Book Citation Index
in Web of Science™ Core Collection (BKCI)

Interested in publishing with us?
Contact book.department@intechopen.com

Numbers displayed above are based on latest data collected.
For more information visit www.intechopen.com

Chapter

Formation of Anticorrosive Structures and Thin Films on Metal Surfaces by Applying EDM

Pavel Topala, Alexandr Ojegov and Vitalie Besliu

Abstract

The methods of the formation of anticorrosive strata and thin films on metal surfaces by applying electric discharge machining (EDM) are presented in this chapter. The increase of anticorrosion resistance of metal surfaces by the formation of palladium depositions, carbon films and oxide and hydroxide films has been demonstrated. Corrosion and electrochemical behaviour of titanium with palladium powder coatings were investigated in sulfuric acid solutions at temperatures of 80 and 100°C. In order to increase the diffusion of palladium in the base material and to increase the layer homogeneity, after coating, the samples were annealed in vacuum at 1150°C for 1 hour. The proposed method allows to reduce the corrosion speed of titanium at least by two orders (from 18.7 to 0.3 g m^{-2} h^{-1}); the corrosion potential is changed towards positive values (from -0.56 mV to $+0.3$ V). The research on surface electrical resistance and resistance to corrosion of oxide and hydroxide films formed on steel C45 surfaces by applying EDM have shown that the surface electrical resistance of the samples increased by 10^7 times, the potential of corrosion increased from -0.44 mV to $+0.4$ V and the resistance to corrosion has increased by about two times in 1% NaCl water solution and by about 10 times in 30% H$_2$SO$_4$ water solution. The less pronounced increase of anticorrosion properties has carbon films formed on the same steel C45 surface; instead they increase superficial microhardness, the functional durability and processing productivity of the active piece surfaces.

Keywords: electric discharge machining, corrosion, thin films, carbon, microhardness

1. Introduction

Corrosion is a damaging process for the absolute majority of parts that work in active environments, from the chemical point of view, and becomes even more pronounced when they operate in energy fields of different types: high temperatures, light, electrical action, etc. It consists in the destruction of metallic materials under the chemical or electrochemical action of the environment or the substances they come into contact with.

With the exception of noble metals, all other metals are unstable in contact with the atmospheric air and aggressive environments. The way this instability manifests

itself, and the degree to which it occurs, depends on the nature of the metal and the environment in which it is placed.

Two types of corrosion can be highlighted considering the deployment mechanism: chemical corrosion [1] which refers to the processes of destruction of metals and alloys produced in dry gases as well as in liquids without electrical conductivity and in most organic substances and electrochemical corrosion [1–8] which causes processes of metal and alloy degradation in electrolyte solutions in the presence of humidity, accompanied by the flow of electric current through the metal.

In all cases, when talking about the functionality of the machines and apparatuses or the parts from which they are assembled and their durability, the process of component degradation of different constructions is a damaging one. Throughout the practical encountered corrosion problems, it is important to know the real speed the process is taking place. If the corrosion process is possible, but has a very low deployment speed, the material is considered corrosion resistant.

Taking into account that iron and its alloys are used in the contemporary construction of machinery and apparatus as basic materials, and, on the other hand, a material for the present and future is considered to be titanium and its alloys, in the following, we will focus on the research of behaviour of these materials in different working environments.

In the case of iron, its corrosion takes place in stages by its oxidation in the atmosphere with the formation of iron oxides (rust).

In the course of the first stage of iron oxidation, FeO is formed, ferrous oxide, which is stable only in the absence of oxygen. When atmospheric oxygen appears, iron oxide is converted into iron hydroxide ($Fe_2O_3 \cdot H_2O$) or $FeO(OH)$, of which two phases are known:

- Phase 1 that corresponds to a large excess of oxygen

- Phase 2 characterized by an insufficient amount of oxygen, which is why oxidation evolves slowly
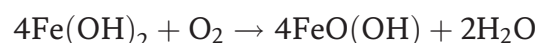
Depending on their colour, there are three types of rust:

1. $Fe(OH)_2$ white rust, formed after the reaction:

$$Fe + 2H_2O \rightarrow Fe(OH)_2 + 2H_2$$
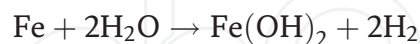
This type of rust quickly passes through oxidation to brown rust, which is why it is rarely seen.

2. Brown rust occurs as a result of the following reaction

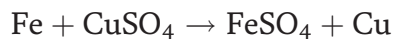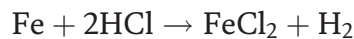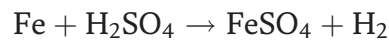$$4Fe(OH)_2 + O_2 \rightarrow 4FeO(OH) + 2H_2O$$

3. The black rust is made of ferrous and ferric oxide, being also called magnetite because of its magnetic properties, and it is considered to be the most stable form of iron oxide. It forms a protective layer on the surface of the metal, with a homogeneous and adherent structure.
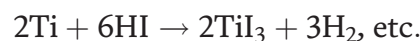
The reaction is as follows:

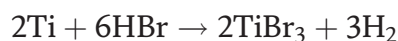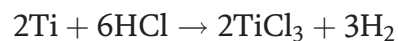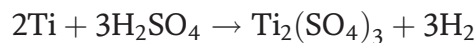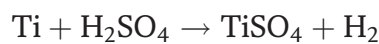$$2FeO(OH) + Fe(OH)_2 \rightarrow Fe_3O_4 + 2H_2O$$

Iron and its alloys are reacted with electrochemically active acids and salts of metals with the destruction of the workpiece surface in working environments:

$$Fe + H_2SO_4 \rightarrow FeSO_4 + H_2$$

$$Fe + 2HCl \rightarrow FeCl_2 + H_2$$

$$Fe + CuSO_4 \rightarrow FeSO_4 + Cu$$

$$Fe + 2NaCl \rightarrow FeCl_2 + 2Na$$

Titanium and its alloys are more resistant to corrosion, since, under normal conditions in the atmosphere, the TiO_2 oxide film is formed, which is stable in different environments, other than those alkaline, for instance:

$$TiO_2 + Na_2CO_3 \, (K_2CO_3) \rightarrow Na_2TiO_3 \, (K_2TiO_3) + CO_2$$
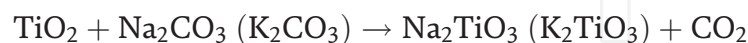
Under certain conditions (high temperature, high concentration), titanium also reacts with some acids:

$$Ti + H_2SO_4 \rightarrow TiSO_4 + H_2$$

$$2Ti + 3H_2SO_4 \rightarrow Ti_2(SO_4)_3 + 3H_2$$

$$Ti + 8HNO_3 \rightarrow Ti(NO_3)_4 + 4NO_2 + 4H_2O$$

$$2Ti + 6HCl \rightarrow 2TiCl_3 + 3H_2$$

$$2Ti + 6HBr \rightarrow 2TiBr_3 + 3H_2$$

$$2Ti + 6HI \rightarrow 2TiI_3 + 3H_2, \text{ etc.}$$

They destroy the base metal and cause further damage of the workpieces in those environments.

The methods and techniques of anticorrosive protection are various and numerous, and they can be grouped into the following categories [9]:

- Methods of preventing corrosion.

- The use of metals and alloys resistant to corrosion.

- Methods of influencing the corrosive medium [10, 11].

- Methods of covering metal surfaces with protective layers [12–14].

- Passivation of surfaces by depositing anticorrosive strata, etc. The essence of preventing corrosion consists in [9].

- Correct choice of materials used in building devices, industrial equipment from the point of view of resistance to corrosion.

- Avoiding the contact of two metals, one of which is more electronegative than the other, e.g., aluminium and copper alloys or alloyed steel, bronze and steel, etc.

- Avoiding the contact of cold-hardened metals with annealed or cast metals, for the reason that due to the difference of electrochemical potential between them, the last one corrodes in the presence of an electrolyte.

- A more careful processing of the metal surface, since hollows and scratches favour and accelerate corrosion.

The group of metals and alloys resistant to corrosion contain noble metals and their alloys, but their use becomes difficult because of the high cost. Self-protective metals and alloys will be used instead. These are metals and alloys which, after an initial corrosion, are covered with an isolating pellicle or film as a result of the passivation phenomenon (e.g. the passivation of Ag in HCl by forming the AgCl film of Fe in HNO_3 concentrated through the formation of the $Fe(NO_3)_3$ pellicle, etc.).

In most cases, metals are alloyed with an adequate component. Sometimes the relatively low concentration of the alloyed component considerably reduces the corrosion speed (e.g., the introduction of such elements as Cu, Cr or Ni of 0.2–0.3% in steels, etc.).

There are many cases when it is possible to influence the corrosive medium to lower the speed of corrosion. There are many possibilities.

The following can be mentioned [9]:

- Modification of pH, which means bringing it to a convenient value for the metal that is to be protected. This consists in the elimination from the medium of corrosion, by the use of physical, chemical and mechanic methods (e.g., neutralization of waste water with chemical substances).

- Removal of gases (O_2 and CO_2), which increase the speed of corrosion in corrosive media, particularly that of the water.

- The use of inhibitory elements (organic or inorganic substances) [10, 11], which, being introduced in small quantities in the corrosive medium, lower or completely annihilate its corrosive capacity.

- Cathode protection (electro-defence) means the use of galvanic methods of metal protection with the help of auxiliary metal anodes, which take over the corrosive capacity of the medium, thus protecting the material used for the workpiece.

The protection realized by applying anticorrosive layers [9, 12–14] means to cover the metal with a thin layer or self-protective material. The self-protective layer should meet the following requirements: it should be compact and adherent, it should be elastic and plastic enough, and its thickness should be uniform in addition to being as small as possible. The protective layer may be metallic or nonmetallic. Metallic deposits may be realized through different methods: galvanic, thermal, through plating, laser radiation, bombarding with ions, alloying by means of electric discharge machining (EDM), etc. The formed surface layers, except those obtained through plating, usually present a certain porosity, which determines the appearance of local portions of corrosion with all the consequences. Nonmetallic protective layers may be organic or inorganic, realized with the help of varnish, paints, enamels or plastic thin sheets.

The formation of inorganic thin films or pellicles (oxide or graphite) on the workpiece surface is a progressive method of anticorrosive protection of superficial layers. The oxide or the graphite, being much more passive than the proper metal, in the interaction with the work media lowers the corrosive potential of the whole piece. The key problem that should be solved is the one that deals with the formation of structurally stable deposits with a high mechanic and electric resistance, having a uniform continuity and thickness on the whole surface.

The choice of the method to be used for the production of the protective layer depends on [9]:

- The conditions and working surroundings of the piece

- The shape and the dimensions of the protective item

- The quality of the supportive material or of the protected item

- The functional technological parameters of the device

- The way the item to be protected is placed in the device

- The technologies of application and executive possibilities for anticorrosive protection

2. Methodology of experimental investigations

2.1 Experimental setup

The experimental setup for the formation of anticorrosive coatings on the metal surfaces of the parts by applying pulsed electric discharge machining (PEDM) comprises the following electric blocks: the power pulse generator, the priming block (intended for initiating the electrical discharge) and the control block, the role of which is to synchronize the power and the priming discharge pulses.

As a result of the specialty bibliographic analysis [12, 13, 15–21], it was concluded that, for the formation of these layers, RC-type generators, with parallel priming, can be successfully used.

The deposition of layers of metallic powders with the use of electric fields is produced as a result of interaction of the powder particles with the plasma jet and the transport of the liquid and vapour phase on the surface of the piece-cathode [12, 13]. The powder particles, having the dimensions of 20–200 μm, are inserted in the 0.3–1.5 mm gap at a capacitor voltage of $U_c = (80...400)$ V.

2.2 Methodology of anticorrosive coatings formation

Research on the interactions of the plasma channel of PEDM with the surfaces of the electrodes have shown that for the phenomenon of electroerosion, two types of effects are characterised as follows: type I, the appearance of the "cold" electrode spots on the electrode surfaces, which give rise to the asperities and impurities on their surface [12, 13] and cause both the cleaning of the surfaces of impurities and their thermal interaction, producing structural changes in the superficial layers of small thicknesses (just about the size of micro- and nanometers), and type II, on the electrode surfaces, in which, after the "cold" electrode spots, the "warm" ones cause the essential melting of the electrode, accompanied by the vaporization phenomena and the dropping of the electrode material [13]. If type II interaction of the plasma channel with electrode surfaces has found a rather wide application in dimensional processing [22–27] and the deposition layer formation (both of the compact materials [21] and the powders [12, 13]), then type I actions are described in the literature only as scientific findings, and for this reason, it is necessary to elucidate the conditions and the effects of surface thermal treatment and to reveal whether this type of interaction is purely thermal or is a thermochemical one.

Analysing the results obtained by the author of the paper [13], it was established that, in order to obtain a type I interaction with the plasma channel (in the absence of surface melting) or type II interaction (when the liquid phase is attested) on the surfaces of the workpieces, it is necessary that the energy density emitted on the processed surface be lower or higher than the specific heat of melting of the material, and the latter can be appreciated by the relation [13, 16, 28]:

$$\frac{4W}{\pi d_c^2 \cdot S} < Q < \frac{4W}{\pi d_c^2 \cdot S}$$

$$Q = q\rho, \tag{1}$$

where q and ρ are the specific heat of melting and the density of the workpiece material, respectively, W is the energy emitted in the gap, d_c is the diameter of the plasma channel and S is the gap value.

As can be seen from the relation (Eq. 1), at the time of the energetic processing regime, the size of the gap and the thermo-physical properties of the workpiece material are known; the diameter of the plasma channel can be determined, which coincides with the size of its trace on the processed surface. If a coefficient of overlapping of the traces (of type I or type II) $k = 0.5...1.0$ and the frequency of the electrical impulses f are known, the productivity of the technological process can be determined by the relation:

$$\eta = \frac{k\pi d_c^2 f}{4} \tag{2}$$

In the paper [13], it has been demonstrated that when PEDM is applied for superficial processing, the erosion processes take place, accompanied by explosive melting and vaporization of the electrode material for the vast majority of studied metals and alloys, for the current pulse duration contained in the limits 10^{-4}–10^{-9} s. It results that, in order to obtain the expected effects, it is necessary to provide a relatively low-duration pulses of discharge.

Effects on electrode surfaces are a function depending on the way of the workpiece connection in the discharge circuit (as anode or as cathode) [13, 16, 21]. These desiderata have been studied in [13], and it has been established that for short-term discharge pulses, they are "cathodic" and for the long-term ones, they are "anodic"; thus, in the case of superficial thermal treatments and deposition of materials, the workpiece will be included in the discharge circuit as cathode. In the case of thermal treatment of steel surfaces, their hardness increases by 2–3 times and for titanium surfaces by 2–5 times, for the formed layers thicknesses from a few micrometres to several dozens of micrometres. The depth of these layers reaches a maximum at three passes of technological cycle for steels and at five passes for titanium and its alloys.

The interaction of the plasma channel with the surface of the electrode workpiece is not always purely thermal; nonetheless the surface of the piece is often enriched with elements contained in the environment and with the contents of the tool-anode material. The penetration depth [13] of these elements in the superficial layer of the piece is a function of both the energy of the discharge pulse and the size of the gap and can be expressed with the relation:

$$h = \frac{kW_S}{AS} \tag{3}$$

where $W_S = \int_0^\tau U(t)I(t)dt$ is the energy emitted in the gap during a singular discharge; U and I are the voltage and the current in the gap, respectively; τ is the

pulse duration; A is the area of the workpiece surface processed at a singular discharge; and k is a constant that depends on the thermo-physical properties of the workpiece material.

2.2.1 Technology of powder deposition formation

From the results of the experimental researches carried out by the authors [12, 13], it has been demonstrated that, in order to obtain the powder depositions, it is necessary to introduce the powder in the anode zone of the gap. From a technological point of view, a parameter that needs to be predicted is the thickness of the deposition layer. This parameter is quite important, because in some cases it is determinant in the technological application of the method. Analysing the experimental results of the authors of this chapter and those of the works [13, 18, 19, 29, 30], in the case of the deposition layers of different materials, the following relationship was deduced for the deposition thickness:

$$H = \frac{P^c \cdot f^d \cdot W^k \left(a - bS^2\right) \cdot r^m}{\rho \cdot A} \cdot n \tag{4}$$

where P is the powder flow, f is the frequency of impulse discharges, r is the equivalent radius of powder particles, W is the energy released in the gap, S is the size of the gap, ρ is the density of the particles' material, A is the area of the processed surface, n is the number of passes of the tool-electrode on the workpiece surface, a and b are individual constants of the deposition materials, and c, d, k, and m are the power exponents that are experimentally established and constitute both functions, of the properties of the powder material and of the processing conditions.

Taking into account the experimental results obtained by the authors of the papers [13, 21] for the determination of the thickness of the deposition layer, the relation (Eq. 4) can be written as

$$H = \frac{\Delta m}{\rho \cdot A} \cdot n \tag{5}$$

where

$$\Delta m = P^c \cdot f^d \cdot W^k \left(a - bS^2\right) r^m \tag{6}$$

The uniformity of deposition of the layer is characterized by the thickness of the deposited layer (or by the dimension Δm on each surface unit). If the processing time is different during the manual processing on different surface portions, the surface is not continuous; the mechanization of the process ensures the formation of uniform deposition on the entire surface of the workpiece.

The compactness of the layers and the existence of recesses or asperities are visually appreciated or measured using the microscope analysis method.

2.2.2 Technology of oxide films formation

In order to achieve the experimental researches, the pulse current generator with priming from a high-voltage block with 12 kV voltage and 0.3 μA current was used; the laboratory installation ensures the positioning, fixing and rotation of the samples during the processing with an adjustable rotation frequency ranging from 0 to 150 rpm [28]. The used tool-electrode was made in the form of cylindrical bar, rounded at the working end in the shape of a hemisphere and made of stainless steel.

The cathode piece was a cylindrical bar 13 mm in diameter. The piece was firmly fixed to the tool-machine frame and the tool-electrode into the tool port. The workpiece was connected to the pulse generator as cathode and the tool-electrode as anode, their axes forming an angle of 90°. In the case of flat surface processing, both the piece and the tool-electrode were made in the form of cylinders with a diameter of 10 mm; they were firmly fixed to the tool-machine port with parallel active surfaces and the electric discharge scanning the workpiece surface by migration of the plasma channel on these surfaces at a processing cycle. The materials for the pairs of electrodes (workpiece/tool-electrode) were chosen: aluminium alloy $AlCu_4Mg_1$, steel C_{45}, titanium alloy $TiAl_6Mo_4$ and copper alloys.

2.2.3 Technology of graphite deposition formation

Experimental research on graphite deposits was carried out under normal conditions in the air environment, under sub-excitation regime of PEDM. For the purpose of realizing the experiments, the power supply having the following parameters was used: the energy released in the gap W_S = 0–4.8 J, the energy accumulated on the capacitor battery W_c = 0–12 J, the voltage on the capacitor battery U_c = 0–200 V, the capacity C = 100–600 µF with step of 100 µF, the gap value S = 0.05–2.5 mm, discharge frequency f = 0–50 Hz and impulse duration τ = 0–250 µs. Due to these parameters, we can provide the PEDM operation under the regime of "hot" electrode spots (with the melting of the processed surfaces) and under the regime of the "cold" electrode spots (without melting the surfaces undergoing processing, although at nanometer scale it occurs).

Between the two electrodes, a graphite cathode and an anode made of the metal specimen, microelectric discharge is applied. The microelectric arc that is produced for a very short period of time—microseconds—has a very high temperature of about $10^{4\circ}$C. At this temperature the graphite erodes (in the form of separated carbon atoms or chemical compounds of the type CO and CO_2 which further decompose into carbon and oxygen, the first being ionized is deposited in the form of film on the metal surface, and the oxygen is released in the plasma [28]), and due to the fact that it is in an electric field, the graphite particles in the vapour state are transported to the opposite sign electrode (anode) made up of the metal specimen. Thus, on the metal surface of the anode, a graphite layer of the micrometre dimension is deposited.

2.3 Methodology for determining the corrosion potential and speed of the samples

In order to measure the potential and the speed of corrosion, a setup was developed, the scheme of which is shown in **Figure 1**. In vessel 1 with electrolyte 2 (3% NaCl water solution for samples made of construction steels and 40% H_2SO_4 water solution for titanium, copper and aluminium alloy samples), the sample and cathode 6 are fixed. The cathode joins at the "−" pole and the sample at the "+" pole of the DC source with smooth voltage regulation. A milliammeter is connected in serial with the source and a voltmeter, in parallel, respectively. To measure the corrosion potential of the superficial oxide layer 4, the base metal 3 is placed in a rubber gasket 5 having a hole 7 so that only the oxidized surface of the sample is in contact with the electrolyte. The voltage is gradually increasing until the current appears, which will be indicated by the voltmeter—the value of the corrosion potential and the milliammeter—the corrosion current. In order to increase the measurement precision, several measurements are made for different parts of the sample surface.
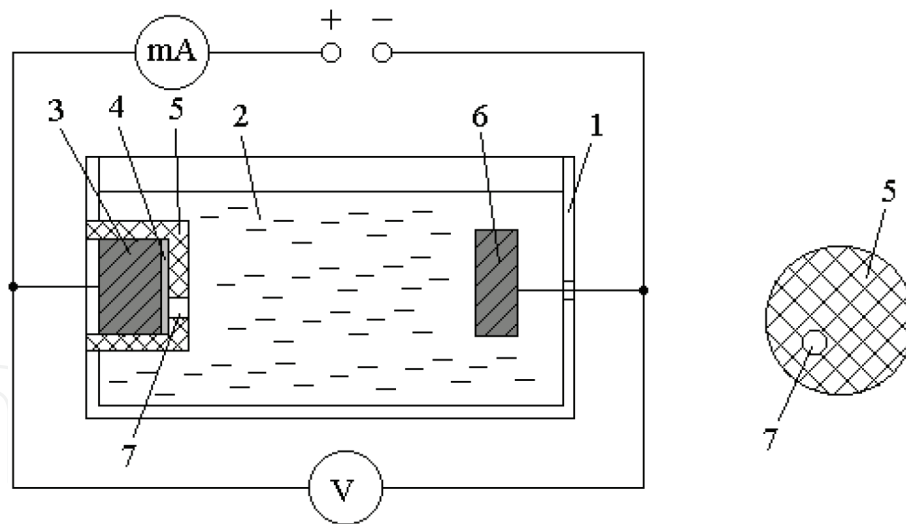
Figure 1.
Potential and speed of corrosion measurement scheme: (1) vessel, (2) electrolyte, (3) sample connected as anode, (4) oxide layer, (5) rubber gasket, (6) cathode and (7) hole for contacting the oxidized surface with the electrolyte in the water solution.

In order to perform the chemical corrosion resistance tests of the processed samples (with PEDM-coated oxide films on the active surface), electrolytes from distilled water and chemical agents with the respective concentration at room temperature were prepared, or, in separate cases, the device was continuously fed with an electrolyte of a certain temperature via a thermostat.

The samples were firmly fixed in the prepared device (**Figure 1**) so that only a circle-shaped part of the processed surface was subjected to dissolution. This was included in the anode dissolution circuit as the anode. The tests were carried out in the operating mode of the experimental DC installation and the 0.1 V step-by-step voltage change [28].

The corrosion speed is determined by weighing the samples before and after the test at the analytical electronic balance KERN ABS-N ABJ-NM with the accuracy of 10^{-5} g.

The corrosion speed index is determined with the relation (Eq. 3):

$$K = \frac{\Delta m}{S \cdot t}; \qquad (7)$$

where K is the speed of corrosion (mass indicator), g·m^{-2}·h^{-1}; S is the area of the workpiece surface, m^2; t is the test duration (work time), h; and Δm is the mass lost (or the mass addition), g:

$$\Delta m = m_i - m_f \qquad (8)$$

where m_i is the initial mass of the sample, g, and m_f is the final mass of the sample, g.

3. Results

3.1 Research on structural and phase transformations in superficial layers of the workpiece

The formation of powder deposition layers is accompanied by a wide range of structural and phase changes [13, 16, 29, 30]. The phase transformations are

conditioned by the occurrence of the liquid phase and the vapour of the deposited particles interacting with the discharge channel, the environment, the cathode material and the liquid phase and solid phase transfer and hardening processes. As it has been shown, due to the electroerosion processes of the cathode material, it may be in the liquid-vapour state and interact with the environment; therefore, usually in the formed powder layer, besides oxides, nitrides and its intermetallic components, cathode material can be introduced in its other phases, respectively [13, 16, 29, 30]. The mentioned phases may occur in the contact zone between the particle and base material during the interaction of the liquid-vapour material of the cathode with the gap medium and the deposited particle and also in the case of deposition of precursor particles, which do not come into direct contact with the material of the piece but which have been influenced by plasma discharge. In particular, this is the area of "cold" spots, whose dimension is larger than the contact area between the sample and the particle (even for the maximum particle diameter of the deposited powder), and this is clearly visible for $S > 0.5$ mm (see **Figure 2**).

The condition in which the deposited particles interact with the surface portion of the workpiece, which has previously been in contact with the plasma discharge, is more often achieved in obtaining the continuous deposition layers.

These conditions were achieved in the roentgen research of the phase component of superficial layers for steels (steel 3, steel C45) and titanium (BT 1-0). Plasma interaction was achieved in the continuous processing (without including the powder in the processing area) when the interaction areas partially or variously overlapped (the number of passes n on the same surface portion varied). The cylindrical electrode-anode was made of graphite. The gap value was changed in the range of 0.15–2 mm, and the other parameters were Uc = 240 V and f = 40 Hz.

The analysis of the change of the phase composition of the processed surfaces (steel C45, titanium BT 1-0) has shown that the basic role in these changes is played by rapid heating and cooling, and their interaction with the environment, during the processing, is not so significant. The intensity of these changes is a function of the deposition material properties and processing conditions, such as the gap value (which, during the experiments, was modified for constant energy emitted in the
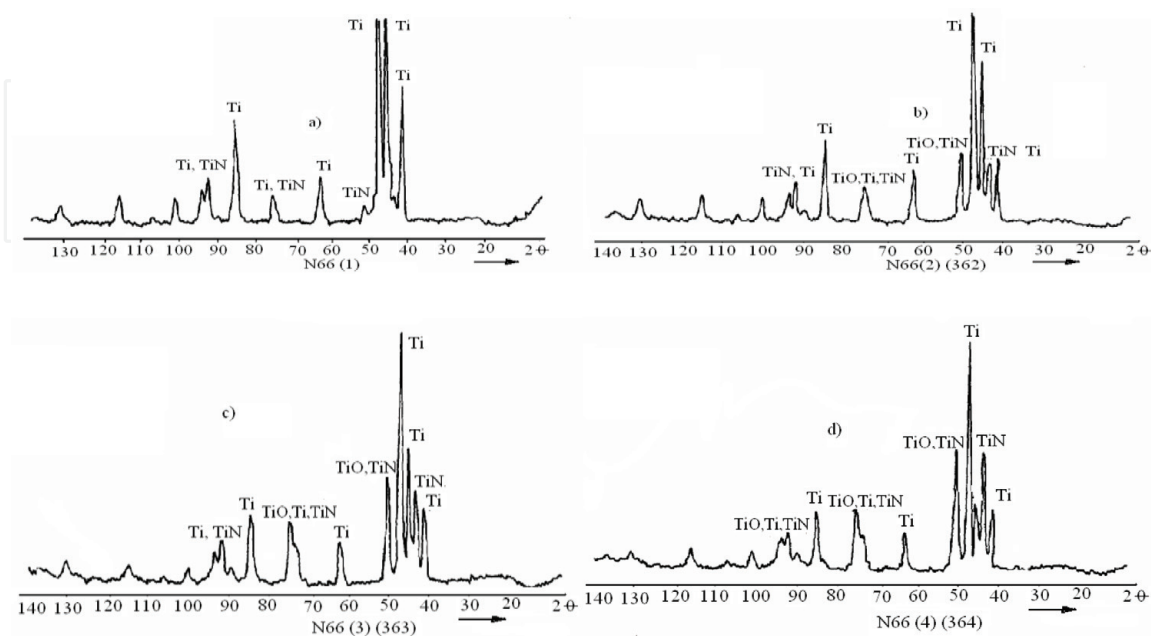

Figure 2.
Diffractograms of titanium BT 1-0 cathode sample surfaces processed by PEDM at a different number of passes, n: (a) 2 passes, (b) 4 passes, (c) 6 passes and (d) 8 passes; the energy emitted in the gap W = 5,3 J; the gap value S = 1.5 mm.

gap W = const). While processing BT-1-0 technical titanium, practically all the phases that are possible in its interaction with the oxygen and nitrogen in the air, under the action of discharge, have been experimented (**Figure 2**) [13]. Oxides (TiO, Ti_2O) and titanium nitride (TiN) form more intensively at gap values S < 1 mm. For larger gaps ($S \geq 2$ mm), only traces of TiO and TiN can be identified (**Figure 2**). In the multiple action of plasma, even for large values of the gap, the same phase component is formed on the surface of the titanium (**Figure 2b**), that is, TiO, TiO_2 and TiN. In this regard, less active is the steel surface; the increase of its processing time (on the account of the number of n passes) changes nonessentially its phase composition (**Figure 3**).

After the action of the discharge plasma on the surface of the steels on the diffractograms, along with the characteristic lines for the ferrite phase, there are also lines corresponding to the austenite phase. The maximum austenite quantity is obtained for $S \leq 0.5$ mm, i.e. when the outbreak surface is practically occupied by the liquid sample material. Some of the lines of the diffractograms can be identified as characteristic to carbide lines (Fe_3C) and to iron nitrides lines (Fe_3N-Fe_4N).

The presence of austenite and cementite lines during the processing of samples made of steel 3 is caused by the transfer on the surface of the anode material (graphite). The absence of oxides for the investigated regimes according to the roentgen method, at first estimation, under normal conditions, confirms the
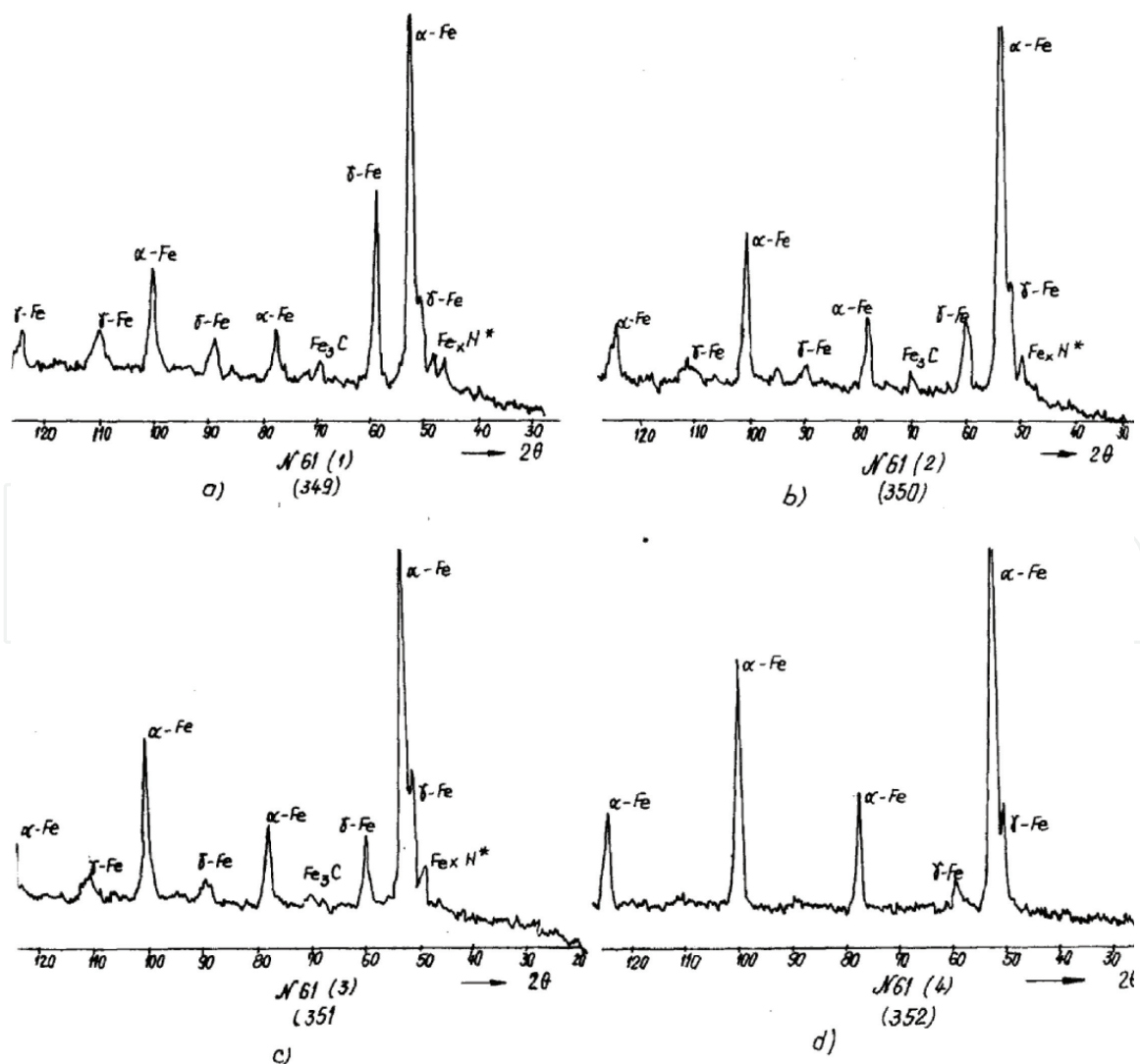

Figure 3.
Diffractograms of steel C45 cathode sample surfaces processed by PEDM for different gap values: S = 0.15 mm (a), S = 0.45 mm (b), S = 1.0 mm (c) and S = 2.0 mm (d).

hypothesis that the "cold" spots burn the oxides and impurities of the superficial layer [31–33], i.e. the discharge channel theoretically "migrates" to these defects of the surface, which finally condition their removal by vaporization (this is valid for singular passes) and also for the reduction of oxides by carbon. The technological process for steel surface cleaning by arc discharge in vacuum is developed based on this phenomenon [34].

The detailed investigations [13] of the processed surfaces using the Mössbauer method of the steel samples (**Figure 4**) indicate both spectra and represent an elusive superposition of iron oxides and hydroxide doublets and confirm the presence of the γ-Fe phase for $S = 0.5$ mm. The distribution of iron, oxygen, carbon and nitrogen in the sample depth is shown in **Figure 5**, which shows that carbon
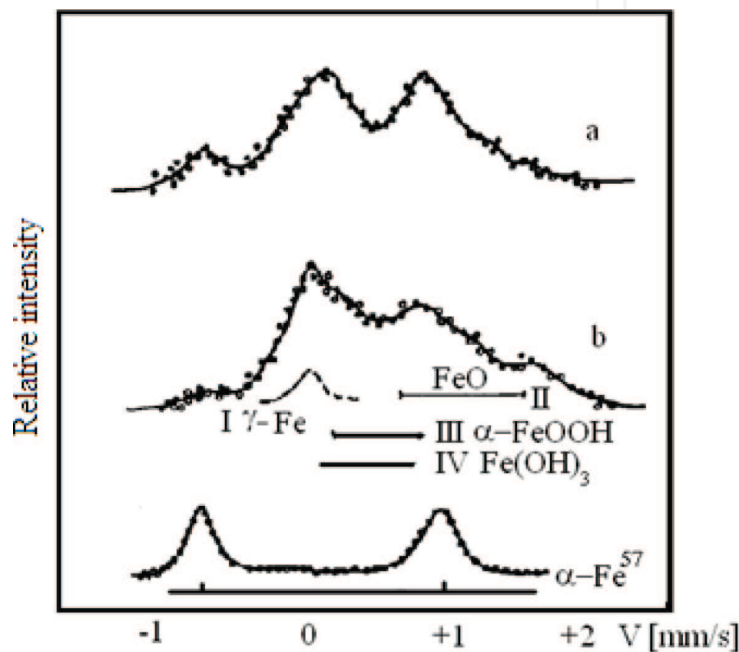

Figure 4.
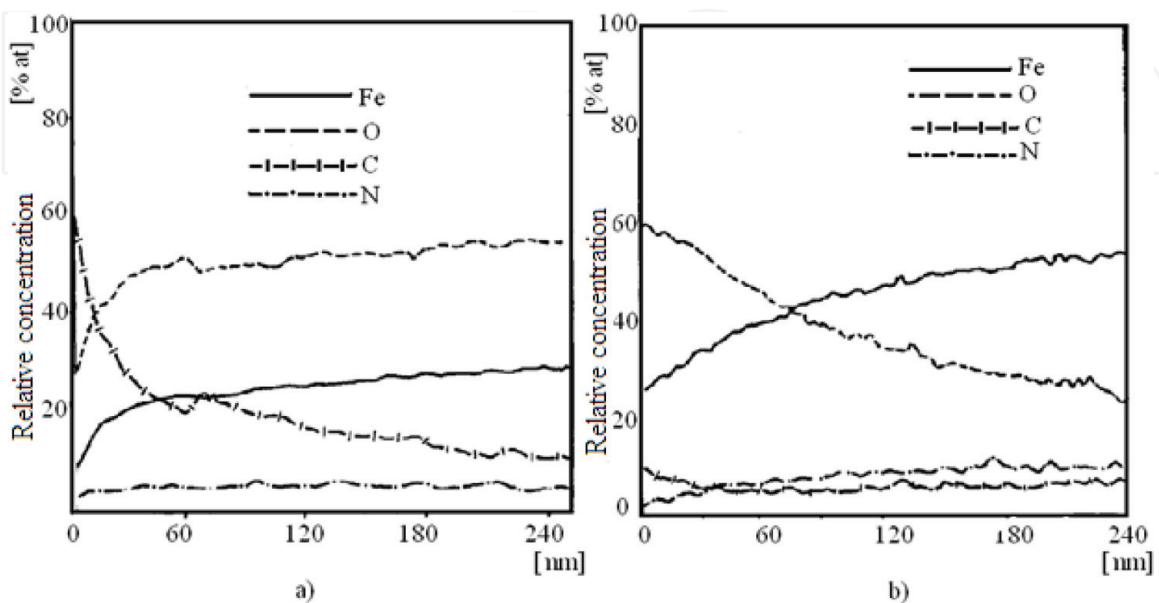*Mössbauer spectra of steel 3 sample after processing by PEDM: S = 2 mm (a) and S = 0.5 mm (b) [13].*

Figure 5.
Elements distribution in steel 3 sample surface after processing by PEDM for gap and specific energy values: S = 0.5 mm and P = 3.19 J·mm^{-3} (a); S = 2 mm and P = 1.5 J·mm^{-3} (b) [13].

aggregates to the surface. Its concentration decreases rapidly as the depth of the investigated layer increases, and the oxygen concentration reaches up to 60%.

This increased oxygen concentration can be achieved in the formation of hydroxides in the superficial layer of the sample. At a depth of layer of up to 240 nm, the nitrogen concentration is up to 5–6%.

For the value of gap S = 2 mm, the main components of the surface are iron and oxygen, and the secondary are carbon and nitrogen, respectively (**Figure 5b**). The oxygen concentration reaches 60% on the processed sample surface and lowers in the depth of the sample; the variation can be explained by the fact that in the superficial layer, hydroxides are formed and, in the depth of the sample, metastable oxides are formed; according to roentgenograms FeO (a single paramagnetic iron oxide at room temperature) is missing on the surface of the sample. Therefore, we can accept meta-stability of some very thin layers of Fe_2O_3 and Fe_3O, which is known according to [13]. Moreover, the possibility of amorphous iron hydroxides formation is not excluded [13]. Mössbauer spectra show that the complexity of unambiguously identifying amorphous hydroxides is very difficult.

The physical composition of the titanium and steel surfaces, after the removal of a layer of 5–10 nm thickness by means of rectification, changes nonessentially: the amount of oxides decreases in titanium and in steels—the nitride component decreases. Changing the energy regime does not condition the essential qualitative changes, for constant values of the gap S = const, and only quantitative changes take place.

Thus, the analysis of diffractograms has shown that among the elements of the processing regimes, the most important that essentially influence the phase compo-nent of the processed surface are the size of the gap, the energy density in it and the time of interaction with the plasma (the impulse duration and the number of passes of the plasma channel on the processed surface).

3.2 Determination of corrosion resistance of titanium and its alloys with deposited layers of metallic powder

In the process of deposition with electrodes made of compact materials by PEDM method, it is difficult to form layers with a full continuity, constant thick-ness, without pores, without impurities, etc., important elements for obtaining corrosion-resistant layers. The depositions obtained by the authors of the papers [13, 16, 29, 30] have shown good results in their corrosion resistance. When depos-iting metal powders, it is possible to form layers with highest thickness, but the problem of porosity remains unresolved.

Up to now, detailed research has been carried out on the corrosion resistance of titanium samples on which palladium (Pd), ruthenium (Ru) and nickel (Ni) depo-sitions have been formed [29, 30]. The modification of the superficial titanium chemical composition with these metals was performed in order to obtain anodes on the base of titanium resistant to corrosion. The obtained results [29, 30] indicate that deposits formed by this method increase the corrosion resistance of titanium by about five times.

The corrosion and the electrochemical behaviour of titanium, with layers formed with the use of metal powders, were investigated by the authors [30] for the application of the 10% H_2SO_4 solution in distilled water at temperatures of 80 and 100°C, respectively. After the formation of the layers, some of the samples were subjected to annealing in vacuum at 1150°C for 1 hour for the purpose of palladium diffusion in the sample material. The corrosion and the electrochemical tests for the annealed samples were carried out in 10% H_2SO_4 solution in distilled water at 80 and 100°C and in 20, 30 and 40% H_2SO_4 solution in distilled water at 100°C. The

palladium content was determined in the solution by the photo-calorimetric method. In the annealed samples, the palladium content was 5.6 mg·cm^{-2}.

The corrosion speed of titanium with powder depositions in 10% H_2SO_4 solution in distilled water at 80°C was 0.2 g·m^{-2}·h^{-1}; at 100°C in the first 5 hours of testing, the speed was 0.78 g·m^{-2}·h^{-1}; and then, during the tests, the speed decreased and, in 50 hours of testing, has dropped to 0.3 g·m^{-2}·h^{-1}. This situation of diminishing the corrosion speed can be caused by the dissolution of the unstable phases in the first hours. The corrosion potential, under these conditions, is situated within the passivity limits and equal to +400 mV in 10% H_2SO_4 solutions at 80°C (relative to the standard hydrogen electrode) and at 100°C equal to +300 mV compared to the titanium samples, without protecting depositions in the 10% H_2SO_4 solution in distilled water, which actively dissolves at potential of -0.56 mV with the speed of 18.72 g·m^{-2}·h^{-1}. Thus, we can state that, in the case of deposits application, the corrosion speed decreases up to 100 times.

After annealing, the corrosion speed has become even smaller.

For 10% H_2SO_4 solution in water at 80°C, this was 0.056 g·m^{-2}·h^{-1}, and at 100°C the corrosion process was completely absent.

With the increase in the solution concentration to 20, 30 and 40% H_2SO_4, respectively, in water, the corrosion rate at 100°C increased accordingly to 0.5, 0.9 and 1.8 g·m^{-2}·h^{-1}. The corrosion potentials, under these conditions, are situated within the passivity limits and are equal to 10% H_2SO_4 solution in water at 80 and 100°C after 5 hours of testing to +700 mV, in addition, corresponding to solutions containing 20, 30 and 40% H_2SO_4 in water; it ranged from +335 to +400 mV (**Figure 6**). For comparison, it can be mentioned that the corrosion speed of Pd layers in 10% H_2SO_4 solution in water at 100°C, depending on the specific processing time and regime, varies from 0.1 to 0.8 g m^{-2} h^{-1}. With increasing acid concentration in water, the speed increases for 40% H_2SO_4 solution at 100°C for different samples, ranging from 0.85 to 2.5 g m^{-2} h^{-1}.
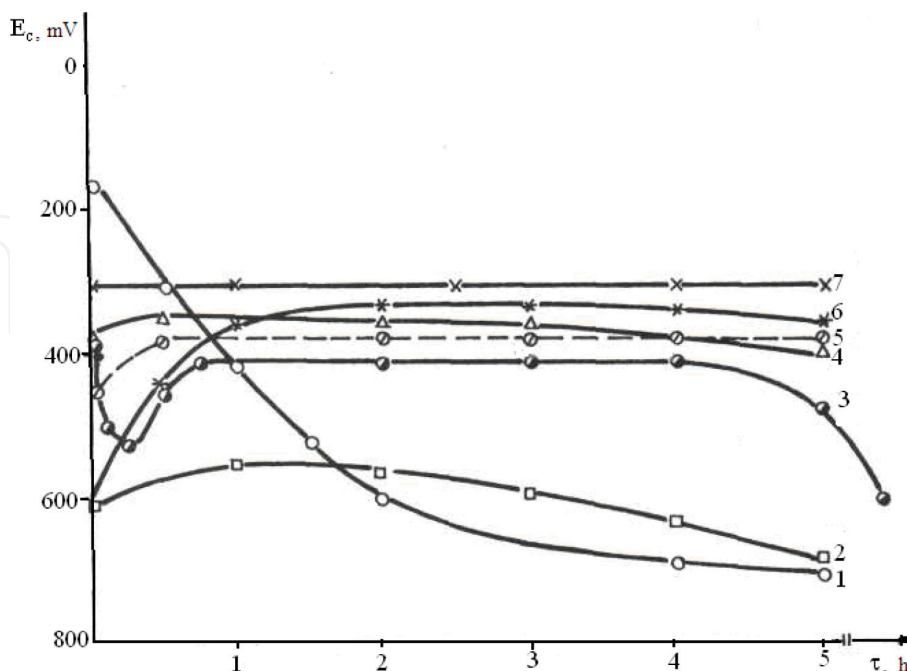

Figure 6.
Changing in time the corrosion potential of palladium-deposited samples (without annealing and after annealing) in water solutions of 10, 20, 30 and 40% H_2SO_4 at 80°C and at 100°C: 1–10% H_2SO_4, 80°C, without annealing; 2–10% H_2SO_4, 100°C, with annealing, 3–10% H_2SO_4, 80°C, without annealing; 4–40% H_2SO_4, 100°C, with annealing; 5–30% H_2SO_4, 100°C, with annealing; 6–20% H_2SO_4, 100°C, with annealing; and 7–10% H_2SO_4, 80°C, without annealing.

The research made by authors, in order to determine the corrosion resistance of titanium and its alloys with the deposited metallic powders, has shown that their corrosion speed can be reduced by 100 times in water solution containing 10–40% H_2SO_4 at the temperature of 100°C, and, in the case of additional subjecting, the annealing process and the corrosion speed can be reduced by more than 100 times, with the intention of homogenizing the structure of the layer and developing the diffusion processes of the elements deposited in the material of the piece. These layers allow to increase the corrosion potential up to +400 mV in 10% H_2SO_4 solution at 80°C and up to +300 mV at 100°C, while the titanium, in the absence of protective depositions, dissolves very actively at the potential of -0.56 mV.

Finally, we can conclude that the deposition of anticorrosive coatings on the surfaces of titanium and its alloy pieces can be applied in the construction of machines, ensuring a considerable duration of their functionality in aggressive environments.

3.3 The results of research on the corrosion properties of oxide films

In the researches carried out by the authors, the results of the experimental measurement of active electrical surface resistance for the samples made of C45 steel, processed by applying PEDM, under atmospheric conditions, at room temperature, are presented both for the surface of the anode-electrode samples and for the surface of cathode workpiece (**Table 1**).

The electrical surface resistance of the unprocessed samples by PEDM plasma ranges from 0.05 to 0.09 Ω mm^{-2}. From the analysis of the experimental results presented in **Table 1**, we can state that, in all cases, there is a substantial increase in the surface active resistance of the electrodes (both of anode and cathode) that participated in the PEDM process, but the active surface resistance of the anode-electrode sample is about three times smaller than that of the cathode-workpiece sample. The last finding can be explained by the fact that at the surface of the anode, under the same conditions, a higher amount of energy is released, and possibly more intense vaporization processes take place, and, on the other hand, the oxygen ions are predominantly directed by the forces of the electric field from the gap to the cathode surface, which is why the intensity of the oxide film formation is less intense on the anode surface.

Sample	Electrical surface resistance, $\times 10^6$ Ω mm^{-2}				
	Experimental data				Average value
Cathode	0.88	0.72	1.46	0.71	0.98
	0.97	1.52	0.68	0.72	
	0.73	1.09	0.76	0.83	
	1.33	1.10	1.04	0.73	
	1.07	0.88	1.21	0.78	
Anode	0.81	0.26	0.46	0.31	0.33
	0.11	0.14	0.56	0.34	
	0.29	0.11	0.62	0.38	
	0.87	0.38	0.11	0.15	
	0.12	0.13	0.27	0.17	

Table 1.
Electrical surface resistance of oxide films for steel C45 samples.

Processed sample material	Average value of surface resistance, $\times 10^6 \ \Omega \ mm^{-2}$
Titanium alloy BT8 (TiAl6Mo4)	1.6
Duralumin Д16 (AlCu4Mg1)	0.25
Technically pure copper M0	0.15
Bronze БрА5 (Cu95Al5)	0.17
Brass Л63 (Cu63Zn37)	0.19

Table 2.
Electrical surface resistance of oxide films formed on the workpiece-cathode surfaces.

Further (**Table 2**), the measurements of the surface electrical resistance of the superficial layer for cathode samples made from titanium, aluminium and copper alloys were made.

As can be seen from the results presented in **Tables 1** and **2**, the electrical surface resistance is a function of the material of the investigated samples and has higher values for the materials with an increased oxygen avidity.

On the basis of the corrosion resistance tests, the volt-ampere characteristic was constructed both for PEDM-treated surface samples under air conditions and for samples with unprocessed surfaces (**Figure 7**).

If we compare the results presented in **Figure 8**, we can see that the anode dissolution potential of the processed sample has increased by six times compared to that of the unprocessed sample. As the voltage applied to the electrodes increases, the anode dissolution table of the investigated pieces changes. For example, in the case of voltage U = 2 V, the current in the circuit for the raw surface is 300 mA, and for the sample with oxide films, it is only 161 mA.

From the volt-ampere characteristic shown in **Figure 8**, we can see that the volt-ampere characteristics for the unprocessed and processed sample in the range 1.5–2.5 V are practically parallel, which shows the presence of an isolation film on the surface of the processed sample which increases its active resistance.

If we take into account the results obtained [28] for the case of measuring the surface active resistance, then we can conclude that the oxide layers formed on the sample surfaces do not have a total continuity, which is why the anodic dissolution process takes place more intensively than we expected.
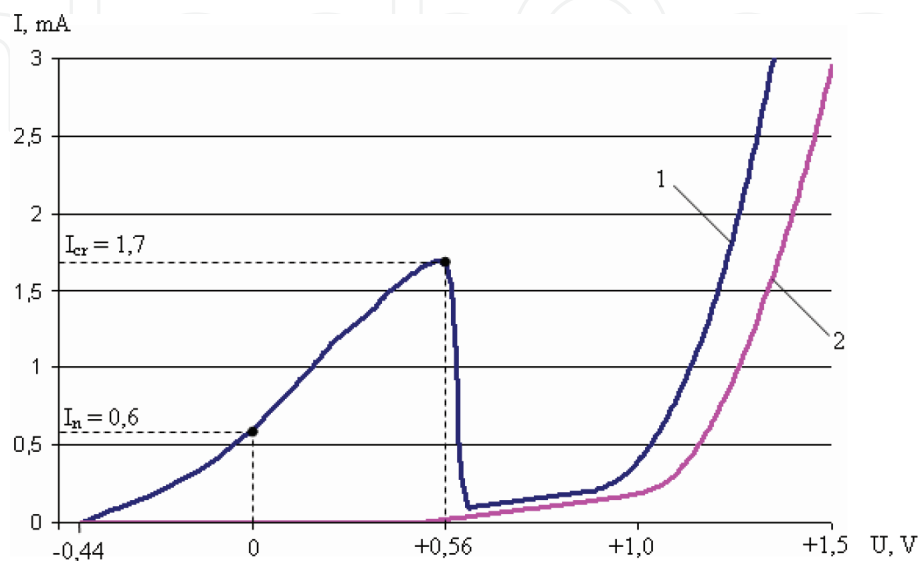
Figure 7.
The volt-ampere characteristic of the corrosion process of the steel C45 samples in the electrolyte (3% NaCl water solution): (1) the raw surface and (2) the processed surface.
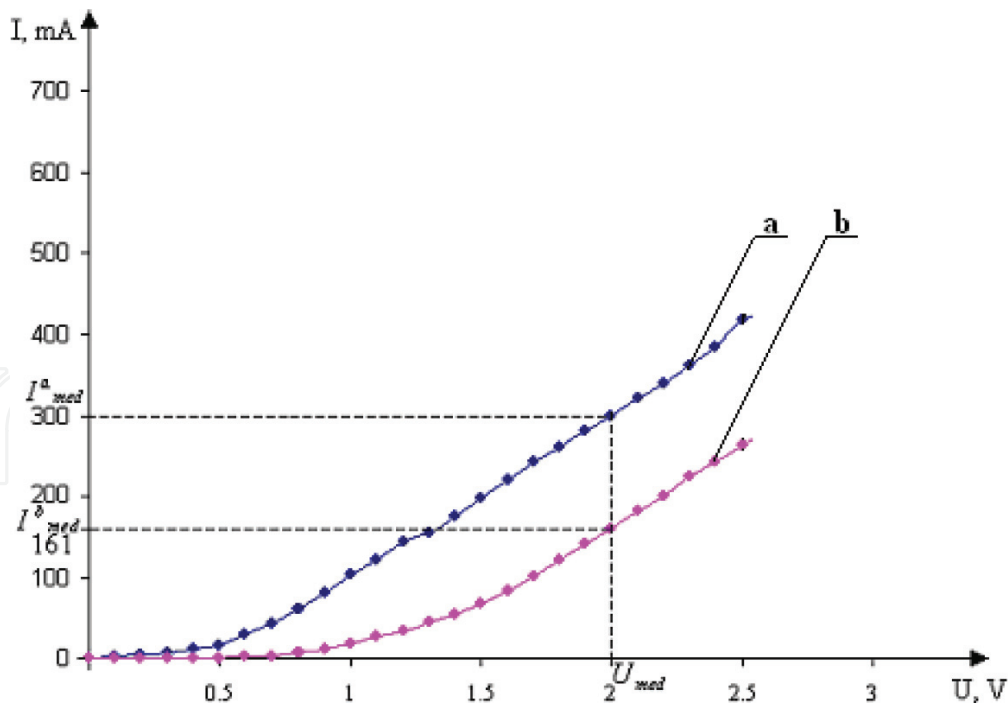
Figure 8.
The volt-ampere characteristic of the electrochemical corrosion process: (a) unprocessed surface and (b) processed surface.

No.	Initial mass of the sample m_i, g	Final mass of the sample m_f, g	Δm, g	Speed of corrosion K, $\mathrm{g\,m^{-2}\,h^{-1}}$
1	12.8441	12.8237	−0.0204	812.10
2	13.1458	13.1254	−0.0204	812.10
3	13.3225	13.3025	−0.0200	796.17
4	14.0610	14.0417	−0.0193	768.31
5	13.0248	13.0031	−0.0217	863.85

Table 3.
Speed of anodic dissolution of steel C45 samples with unprocessed surfaces [28].

No.	Initial mass of the sample m_i, g	Final mass of the sample m_f, g	Δm, g	Speed of corrosion K, $\mathrm{g\,m^{-2}\,h^{-1}}$
1	12.8569	12.8441	−0.0128	509.55
2	13.1605	13.1458	−0.0147	585.19
3	13.3338	13.3225	−0.0113	449.84
4	14.0717	14.0610	−0.0107	425.95
5	13.0366	13.0248	−0.0118	469.74

Table 4.
Speed of anodic dissolution of steel C45 samples with oxidized surfaces [28].

For the purpose of determining the corrosion speed, five pairs of unprocessed and processed by PEDM plasma samples were subjected to testing under the same anodic dissolution conditions. Based on the measurements, **Tables 3–6** were completed.

If we analyse the obtained results, we can see that, for the case of processed samples made of C45 steel, the corrosion speed in 3% NaCl water solution, at the applied voltage of 2 V, is, practically in all cases, twice lower than for the

No.	Initial mass of the sample m_i, g	Final mass of the sample m_f, g	Δm, g	Speed of corrosion K, $\text{g m}^{-2}\,\text{h}^{-1}$
1	1.6803	1.6700	−0.0103	103
2	1.6700	1.6599	−0.0101	101
3	1.6599	1.6466	−0.0133	133
4	1.6466	1.6324	−0.0142	140
5	1.6324	1.6198	−0.0126	126

Table 5.
Speed of anodic dissolution of titanium BT8 samples with unprocessed surfaces.

No.	Initial mass of the sample m_i, g	Final mass of the sample m_f, g	Δm, g	Speed of corrosion K, $\text{g m}^{-2}\,\text{h}^{-1}$
1	1.9582	1.9578	−0.0004	4
2	1.6615	1.6613	−0.0002	2
3	1.8829	1.8828	−0.0001	1
4	1.8325	1.8324	−0.0001	1
5	1.7648	1.7647	−0.0001	1

Table 6.
Speed of anodic dissolution of titanium BT8 samples with oxidized surfaces.

unprocessed samples by oxidation. The speed of corrosion of titanium samples with oxide films in 30% H_2SO_4 water solution at 80°C decreases by about 100 times comparatively with the unprocessed titanium surfaces.

If it is taken into account that the potential for natural corrosion is tens and hundreds of times less than in the case of the tests carried out, then the effectiveness of the application of oxides and hydroxides, in the amorphous state, will increase more significantly. For example, if we return to **Figure 7**, then we can see that, for the voltages applied in the limits of 0 and +0.4 V, the current in the circuit, formed by the workpiece, does not exist; consequently, the corrosion speed will be zero, whereas, under the same conditions, for the raw piece, there are considerable currents; therefore, the corrosion speed is significant. Finally, we can admit that the application of amorphous oxides and hydroxides to metal surfaces by PEDM is beneficial for increasing their active corrosion resistance.

3.4 The corrosion resistance of the graphite film

In order to determine the corrosion resistance of the graphite films, the method of electrochemical research was chosen. This method was used because it allows the acceleration of the corrosion process, which is nothing more than anodic dissolution, and, thus, it shortens the study of a sample [28].

The electrochemical installation is composed of an electrolysis cell containing a 1% NaCl water solution in which two electrodes are placed, a steel cathode and anode, also made of steel or graphite film-coated steel. They are connected by a voltmeter and an ampere metre at an adjustable DC source in the range of 0–40 V [28].

In order to determine the value for the potential of the electrochemical dissolution, it is necessary to build the volt-ampere characteristic, for the sample anode steel C45 and for the sample anode steel C45 covered with graphite. The cathode material, in both cases, is steel C45.

For the beginning, the samples were polished and rinsed with distilled water, then placed in the electrolyte solution at a distance of 10 mm one from another. A DC voltage, with an 0.4 V increments, is applied at a holding time of 3 min (**Figure 9**). The values for the electric currents are recorded by the ammeter, and they are presented in **Figure 9**.

When samples are placed in electrolyte, in the absence of external electric current, a stationary potential is established.

In the case when both electrodes are made from the same type of steel, the stationary potential is almost zero, and, in the case when the anode is covered with graphite, the stationary potential is 0.1 V.

When an external potential is applied, curves are obtained (**Figure 9** (curve 2)). It is observed that, for the steel sample, with the increasing potential, an increase in current intensity occurs as well, up to the value of 2 V, followed by an area where a decrease of intensity occurs up to the value of 2.9 V.

This effect may be due to the oxidation and hydroxylation chemical reactions that lead to the steel surface passivation, in the absence of the graphite film.

After this value, as shown in the chart, with the increase in the potential difference, the corrosion current decreases, and the corrosion process takes place at low speed, i.e., passive film emerges, which does not allow anodic dissolution.

The passive state is maintained until the potential of 2.8 V; then the current intensity increases considerably, accelerating the corrosion process.

An analogue behaviour is found while researching the graphite-coated steel sample, excluding that the passivation area appears almost at the value of 5.6 V.

Within the field of 5.6–6.2 V, the destruction of the deposited graphite film is observed, followed by an increase of corrosion currents.

The performance of the sample, covered with graphite film (**Figure 10**, curve 1), demonstrates that the presence of carbon significantly enhances the surface potential of the passivation ~3.2 V.

It is possible that the presence of graphite on metallic electrode surface generates deoxidation reactions, and the porosity of graphite film ensures the electrical contact between the electrolyte environment and the sample surface.

In **Figure 10**, the corrosion rate variation, depending on the time of immersion, is shown for the samples processed with graphite electrode tool.

From the analysis results, related to corrosion speed variation, depending on the duration of samples exposure in aggressive environment (**Figure 10**), we can
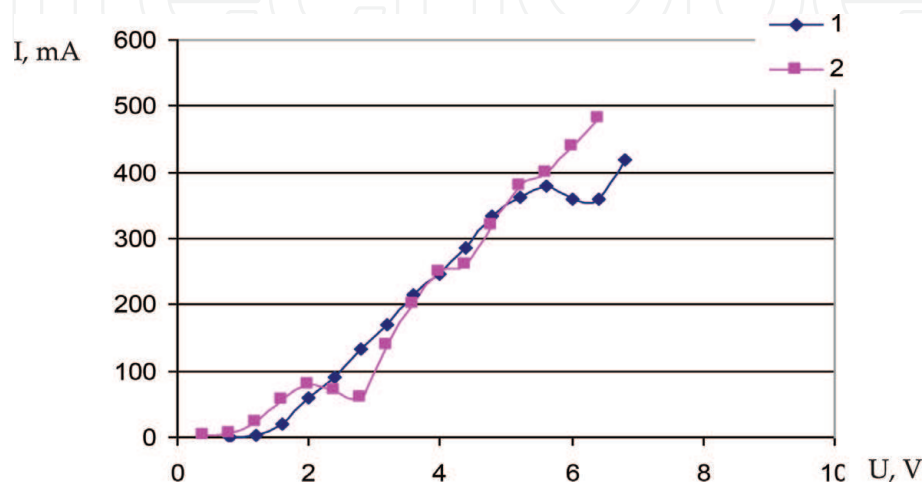

Figure 9.
Volt-ampere characteristic for the electrochemical process [28]: (1) steel C45 covered with graphite and (2) unprocessed steel C45 surface.
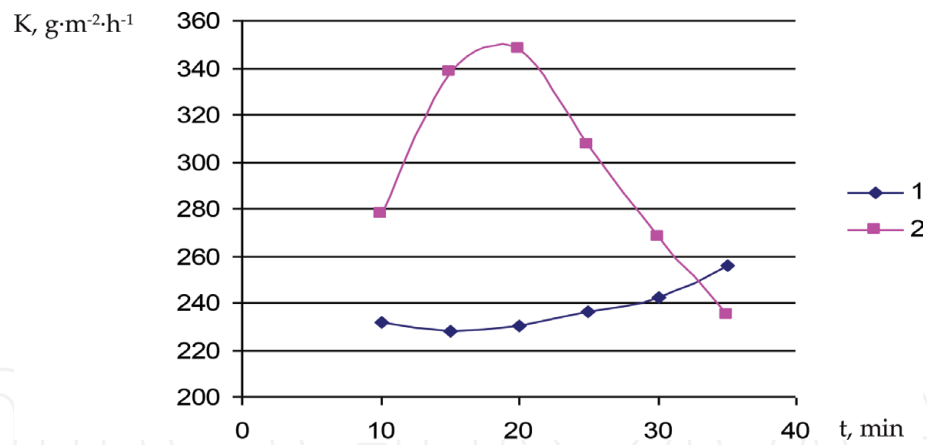
Figure 10.
Corrosion speed variation depending on the time of immersion [28]: (1) steel C45 covered with graphite and (2) unprocessed steel C45.

outline essentially higher corrosion rates for the initiation stage of corrosive process, in the case of unprocessed steel 45 without a graphite pellicle (**Figure 10**, curve 2).

Afterwards, with the passing of time, the process of corrosion is attenuated; the determined corrosion rate is smaller, when the time of immersion is longer.

Similarly, with the passing of time, the nature of the corrosion product is modified; oxides are most likely formed, having a low oxygen content and being more stable (Fe_3O_4) ($FeO \cdot Fe_2O_3$).

Simultaneously, it is acceptable that corrosion products form films on the metal surface that insulate the metal from corrosive agents. For this reason, the curves showing the variation of corrosion rate time show a trend of flattening.

These films are adherent and also compact enough so that the corrosion process diminishes in time, but does not annihilate.

It should be noted that the determinations were made in a static regime. In dynamic conditions, the formed oxide film can probably detach from the metal surface, and, in this case, the corrosion process is conducted with higher corrosion rates.

In the case of steel coated with graphite film, lower corrosion rates are found; afterwards, they begin to rise due to degradation of graphite film, as a result of its destruction.

Experimentation established that in acid solution of 30% HNO_3, after 3 min, the amount of uncovered graphite steel electrochemically dissolved 1.4 times greater than graphite-coated steel—1.3 times greater in 10 min. In salt solution of 1% NaCl, the amount of uncovered graphite steel electrochemically dissolved was 1.2–1.4 times greater than graphite-coated steel deposited by PEDM.

4. Conclusions

Analysing the results of the experimental researches, we can conclude the following:

- Thermal treatment, in the absence of liquid phase formation on the processed surface, can be performed only in the regime of maintenance of the electrical discharge in impulse on "cold" electrode spots.

- Under superficial processing conditions, with the maintenance of electric spell released on "cold" electrode spots, the mass transfer in the solid phase can

reach depths of dozens of μm diameters, which will allow the working surfaces of the parts and cutting tools of the layers with prescribed physico-mechanical properties that will provide them with high-performance features.

- The thermal and chemical-thermal processes that result in the surface layers of the parts under the action of the plasma channel of the electrical discharges in impulse cause not only the modification of their chemical composition but also the modification of their physico-mechanical properties.

- Oxide films, formed as a result of interaction with PEDM plasma, increase the resistance by 10^6–10^7 times, which, in turn, influences the corrosion resistance.

Author details

Pavel Topala*, Alexandr Ojegov and Vitalie Besliu
Alecu Russo Balti State University, Balti, Republic of Moldova

*Address all correspondence to: pavel.topala@gmail.com

IntechOpen

References

[1] Nanu A. Technology of Materials. Chisinau: Ştiinţa; 1992. 552 p

[2] Tian BR, Cheng YF. Electrochemical corrosion behaviour of X-65 steel in the simulated oil sand slurry. I: Effects of hydrodynamic condition. Corrosion Science. 2008;**50**(3):773-779

[3] LiuYing L, FuhuiWang L. Electrochemical corrosion behaviour of Nano crystalline materials: A review. Journal of Materials Science and Technology. 2010;**26**(1):1-14

[4] Rihan RO. Electrochemical corrosion behaviour of X52 and X60 steels in carbon dioxide containing saltwater solution. Materials Research. 2013;**16**:1 Epub Dec 04, 2012

[5] Kuphasuk C, Oshida Y, Andres CJ, Hovijitra ST, Barco MT, Brown DT. Electrochemical corrosion of titanium and titanium-based alloys. The Journal of Prosthetic Dentistry. 2001;**85**(2): 195-202

[6] Huang C-L, Chen T-H, Chiang C-C, Lin S-Y. Electrochemical corrosion and mechanical properties of two biomedical titanium alloys. International Journal of Electrochemical Science. 2018;**13**:2779-2790. DOI: 10.20964/2018.03.26

[7] Song G-L. The grand challenges in electrochemical corrosion research. Frontiers in Materials. 2014. DOI: 10.3389/fmats.2014.00002

[8] Tian G et al. Investigation on electrochemical corrosion characteristic of 2A14 aluminum alloy in nitric acid. Surface Review and Letters. 2017; **24**(1850016):10. DOI: 10.1142/ S0218625X18500166

[9] Topala P, Ojegov A. Formation of oxide thin pellicles by means of electric discharges in pulse. Annals of the Oradea University. Fascicle of Management and Technological Engineering. 2008. CD-ROM Edition. Edition of University from Oradea, Romania. ISSN 1583-0691, CNCSIS "Class B+";**VII**(XVII):1824-1829. DOI: 10.15660/AUOFMTE.2008.1213

[10] Negm NA, Salem MA, Badawi AM, Zaki MF. Corrosion inhibition properties of some novel n-methyl diethanolammonium bromide cationic surfactants. TESCE. 2004;**30**(2):853-869

[11] Gogoi PK, Barhai B. Corrosion inhibition of carbon steel in open recirculating cooling water system of petroleum refinery by a multi-component blend containing zinc(II) diethyldithiocarbamate. Indian Journal of Chemical Technology. 2010;**17**: 291-295

[12] Topala P. Cercetări privind obţinerea straturilor de depunere din pulberi metalice cu aplicarea descărcărilor electrice în impuls. In: Rezumatul Tezei de Doctorat. Bucureşti: Universitatea Politehnica; 1993. p. 32

[13] Topală P. Cercetări privind obţinerea straturilor de depunere din pulberi metalice cu aplicarea descărcărilor electrice în impuls. In: Teza de Doctorat în tehnică. Bucureşti: Universitatea Politehnica; 1993. p. 161

[14] Abdulkareem MAA, Hani AA. The effect of zinc, tin, and Lead coating on corrosion protective effectiveness of steel reinforcement in concrete. American Journal of Scientific and Industrial Research. 2011;**2**(1):89-98. ISSN: 2153-649X. DOI: 10.5251/ ajsir.2011.2.89.98

[15] Topală PA, Balcănuţă NP. Caracteristicile electrodinamice ale descărcărilor electrice în impuls. In: Tehnologii Moderne, Calitate, Restructurare. Chişinău: Universitatea Tehnică a Moldovei; 2001. pp. 203-208

[16] Topala P. Conditions of thermic and thermo-chemical superficial treatment innards with the adhibition of electric discharge in impulses. In: Nonconventional Technologies Review. Bucureşti: Editura BREN; 2005. pp. 27-30

[17] Topală P. Aplicări ale electroeroziunii în dezvoltarea tehnologiilor fine de prelucrare superficială a pieselor. Analele Ştiinţifice ale Universităţii de Stat "Alecu Russo" din Bălţi.—Serie nouă. Fasc. A. 2004. Tom XX, p. 66-69

[18] Топала ПА, Гитлевич АЕ, Корниенко ЛП. Коррозионное поведение титана с электроискровыми покрытиями. Москва: Защита металлов, 1989, vol. 29, № 3, pp. 351-356

[19] Топала Пи др. Влияние отжига на коррозионное поведение титана с электроискровыми покрытиями. Москва: Защита металлов. 1990. vol. 26. № 3. pp. 433-437

[20] Топала П и др. Упрочнение металлических поверхностей на участках для электроискрового легирования. In: Машиностроение и техносфера Xxi века. Vol. 3. Донецк: Сборник трудов XIII Международной научно-технической конференции; 2006. pp. 262-265

[21] Topală P, Stoicev P. Tehnologii de Prelucrare a Materialelor Conductibile cu Aplicarea descărcărilor Electrice în Impuls. Chişinău: Editura Tehnica-Info; 2008. p. 265

[22] Парканский НЯ. Исследования процесса электроискрового нанесения покрытий из порошковых материалов в электрическом поле. Дис. канд. техн. наук. Киев: Институт проблем материаловедения АН УССР; 1979. p. 27

[23] Ливурдов ВИ и д. Структура и эксплуатационные свойства деталей с покрытиями, полученными электроискровым легированием порошковыми материалами. ЭОМ. 1980; (5):33-35

[24] Парканский НЯ, Гитлевич АЕ. Особенности поверхности слоев катода при электроискровом нанесении порошковых материалов. ЭОМ. 1981; (1):32-35

[25] Гитлевич АЕ и д. Электроискровое легирование металлических поверхностей. Кишинев: Штиинца; 1985. p. 196

[26] Немошкаленко ВВ и др. Особенности формирования поверхностных слоев при искровых разрядах. Киев: Металлофизика. 1990. vol. 12. № 3. pp. 132-133. ISSN 0204-3580

[27] Мицкевич МК и др. Электроэрозионная обработка металлов. Минск: Наука и техника. 1988. p. 216

[28] Tiginyanu I, Topala P, Ursaki V, editors. Nanostructures and Thin Films for Multifunctional Applications. NanoScience and Technology. Switzerland: Springer International Publishing; 2016. p. 576 p. ISSN 1434-4904, ISBN 978-3-319-30197-6. DOI: 10.1007/978-3-319-30198-3

[29] Корниенко ЛП и др. Электрохимическое и коррозионное поведение титана с электроискровыми покрытиями Pd и Cr-Pd. Москва: Защита металлов. 1991. vol. 29. № 3. pp. 351-358

[30] Chernova GP et al. The influence of annealing on the corrosive behaviour of titanium with electrospark palladium surfaces. Metal Protection. 1990;**26**(3): 433-437

[31] Любимов ГА, Раховский ВИ. Катодное пятно вакуумной дуги. УФН. 1978;**125**(4):665-706

[32] Бушик АИ. Исследование динамики процессов при импульсном разряде на сложных электродах. Автореф. дис.

канд, ф.-м. наук. Минск: ФТИ АН БССР. 1973. p. 23

[33] Антонов СА и д. Дуговая эрозия катодов, содержащих включения эмиссионноактивной фазы. ЖТФ. 1982; **52**(52):266-270

[34] Булат ВЕ, Эстерлив МХ. Очистка металлических изделий от окалины, окисной плёнки и загрязнений электродуговым разрядом в вакууме. ФХОМ. 1987;(3):49-53